1^1B_u (S_2) and 2^1A_g (S_1) Fluorescence and the 2^1A_g State of α,ω-Dithienylbutadiene and α,ω-Dithienylethylene

Takao Itoh*,† and Minoru Yamaji‡

Graduate School of Integrated Arts and Sciences, Hiroshima University, 1-7-1 Kagamiyama, Higashi-Hiroshima City, 739-8521 Japan, and Department of Chemistry, Graduate School of Enginering, Gunma University, Kiryu, 376-8515 Japan

Received: May 24, 2008; Revised Manuscript Received: October 02, 2008

Fluorescence and absorption spectra and fluorescence lifetimes have been measured for α,ω-dithenylbutadiene (DTB) and α,ω-dithenylethylene (DTE) in different solvents and at different temperatures as well as in the vapor phase. It is shown that the emission of DTB consists of the S_2 (1^1B_u) and S_1 (2^1A_g) fluorescence, while the emission of DTE consists of solely the S_1 (1^1B_u) fluorescence. The 2^1A_g and 1^1Bu state levels of DTB are found to invert in solvents with the polarizability of near 0.32. All the available data for DTB on temperature and solvent dependence of the absorption and fluorescence spectra and the fluorescence lifetime support the presence of the lowest excited singlet state, 2^1A_g, located below the strongly allowed 1^1B_u state. Quantitative analyses of the spectral data provide the physical parameters that characterize the excited state dynamical behavior of DTB.

1. Introduction

Linear polyenes are typical π-conjugation molecules and are known for the intense absorption originating from an optically allowed singlet state of the B_u symmetry. Fundamental revision of the electronic structure of linear polyenes has been made since the discovery of the optically forbidden singlet state of the A_g symmetry located at energies below the strongly allowed ^1Bu state.[1−3] The presence of the forbidden 2^1A_g state at energies below the allowed 1^1B_u state has been verified for a number of polyenes including unsubstituted, α,ω-dimethyl, and α,ω-diphenylpolyenes.[1−9] Detailed information on the electronic structure of linear polyenes is the foundation for understanding complicated processes such as the charge transport in conducting polymers as well as the energy transfer in biological systems.

Because of the high stability and high fluorescence quantum yield, diphenylpolyenes have been used for a number of spectroscopic investigations. The measurements of the fluorescence spectra for diphenylpolyenes with 3 through 7 double bonds in the polyene chain in solution and those with 2 through 4 double bonds in the vapor phase revealed the presence of the dipole forbidden 2^1A_g state located below the strongly allowed 1^1B_u state.[2,4,5,7,8,10] α,ω-Dithienylpolyenes also can be regarded as substituted linear polyenes and the fluorescence and excitation spectra have been reported for these polyenes with 2 through 4 double bonds in the polyene chain in low temperature *n*-alkane matrices.[11] These spectra showed the presence of the dipole forbidden 2^1A_g state for dithienylpolyenes, although the 2^1A_g and 1^1B_u states are nearly degenerate for α,ω-dithenylbutadiene (DTB) in low-temperature matrices.[11] To reconfirm the presence of the forbidden 1^1A_g state for thienylpolyenes and to compare the photophysical properties of thienylpolyenes with those of other polyenes, we have investigated the spectroscopic properties under different conditions.

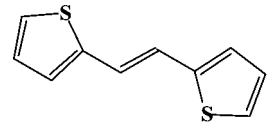

1, 2-di(2-thienyl)ethylene (DTE)

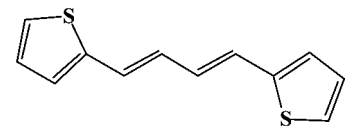

1, 4-di(2-thienyl)-1, 3-butadiene (DTB)

In the present work, fluorescence, fluorescence excitation and absorption spectra, and fluorescence lifetimes have been measured for *trans*-1,4-di(2-thienyl)-1,3-butadiene (DTB) and *trans*-1,2-di(2-thienyl)ethylene (DTE) in solvents with different polarizabilities and at different temperatures as well as in the vapor phase. It is shown that the 1^1B_u (S_2) fluorescence appears as a weak emission band on the high-energy side of the 2^1A_g (S_1) fluorescence for DTB in room temperature solution and in the vapor phase, while only the 1^1B_u (S_1) fluorescence appears for DTE. That is, in most of the room temperature solutions the lowest excited singlet state S_1 is assigned to 2^1A_g for DTB and to 1^1B_u for DTE. The 2^1A_g and 1^1Bu state levels of DTB invert in solvents with the polarizability of near 0.32. By measuring and fitting the temperature and solvent-polarizability dependence of the fluorescence and absorption spectra and the fluorescence lifetimes quantitatively, we were able to show that the weak emission originates from the S_2 (1^1B_u) state, which is in thermodynamic equilibrium with the S_1 (2^1A_g) state.

2. Experimental Section

1,4-Di(2-thienyl)-1,3-butadiene (DTB) and 1,2-di(2-thienyl)ethylene (DTE) obtained from Tokyo Chemical Industry were purified by means of repeated recrystallization first from acetone and second from carbon tetrachloride. It was confirmed that the excitation spectrum agreed well with the corresponding absorption spectrum. The solvents used are all of spectroscopic grade.

Vapor-phase samples were prepared on an all-glass vacuum line. Perfluorohexane sealed in a sidearm was degassed by repeated freeze−pump−thaw cycles. The use of perfluorohexane as a buffer gas is due to the chemical stability and temperature

* Corresponding author. E-mail: titoh@hiroshima-u.ac.jp.
† Hiroshima University.
‡ Gunma University.

10.1021/jp804592m CCC: $40.75
Published on Web 11/24/2008

as well as due to the absence of absorption in the UV region. Further, the pressure of perfluorohexane can be changed easily in a wide range from 1 up to 200 Torr at room temperature by changing the temperature of the sidearm of the reservoir. A small amount of sample crystal in a quartz cell sealed to the vacuum system was heated to 80 °C at a background pressure of less than 10^{-4} Torr to remove volatile impurities such as water. The buffer gas was admitted into the sample cell after degassing. The pressure of the buffer gas was controlled by the temperature of the sidearm, which was varied from −20 to 0 °C. The sample cell with buffer gas was then isolated from the buffer gas reservoir, the contents were trapped by liquid nitrogen, and the cell was sealed off. By measuring the pressure and volume of the buffer gas before trapping and by measuring the volume of the cell at the end of the experiment, we estimated the buffer gas pressure.

The temperature of the sample cells for vapor samples was controlled by a thermostated cell holder that consists of lower and upper parts. The lower part covers most of the quartz square cell for which the emission is detected. The temperature of the lower part of the sample cell was kept at 150 °C and that of the upper part was kept at 147 °C.

Absorption spectra were measured with a Shimadzu UV-2550 spectrophotometer, and emission and excitation spectra were measured with a Hitachi F-4500 or a Spex Fluorolog-3 (Model 21-SS) spectrophotometer. The latter spectrophotometer is equipped with a double-grating excitation monochromator, a high-pressure 450-W Xenon lamp as an excitation-light source, and a photomultiplier tube (Hamamatsu R928-P) in an electric-cooled housing operated in photon-counting mode. For most of the measurements square 10-mm path length quartz cells were used, but a cylindrical quartz cell with a 100-mm path length was also used for measurements of weak absorption.

Fluorescence lifetimes in the nanosecond region were measured with a time-correlated single-photon counting fluorimeter (Edinburgh Analytical Instrument FL-900CDT), while the fluorescence lifetimes in the picosecond region were measured with a femtosecond laser system equipped with a mode-locked Ti:sapphire laser (Spectra-Physics, Tsunami; the center wavelength 800 nm, pulse width of about 70 fs, and repetition rate of 82 MHz) pumped by a CW green laser (Spectra-Physics, Millenia V; 532 nm, 4.5 W). The repetition frequency was reduced to 4 MHz by using a pulse picker (Spectra-Physics Model 3980) and the third harmonics (266 nm, fwhm ca. 250 fs) was used as the excitation light source. The monitoring system consists of a microchannel plate photomultiplier tube (MCP-PTM; Hamamatsu, R3809U-51) cooled at −20 °C and a single-photon counting module (Becker and Hickl, SPC-530). The fluorescence signal detected by MCP-PTM and the photon signal of the second harmonics (400 nm) of the Ti:sapphire laser were used for the start and stop pulses of a time-to-amplitude converter in the system, respectively. The instrumental response function had a half-width of about 25 ps. The fluorescence decay profiles were analyzed with use of the deconvolution method.

Fluorescence spectra were corrected for the spectral sensitivity of the detection system by comparing the measured spectrum with the real spectrum, using *N*,*N*-dimethylnitroaniline as a standard which shows the emission ranging from 12 000 to 22 000 cm^{-1} in a hexane−benzene mixture. Fluorescence spectra ranging from 18 000 to 25 000 cm^{-1} were corrected by using quinine in sulfuric acid as a standard. Excitation spectra were corrected for the spectral intensity distribution of the exciting light with use of an aqueous solution of rhodamine B as a quantum counter. Fluorescence quantum yields were determined by a relative method by using a solution of quinine in sulfuric acid as a standard, assuming that the quantum yield of the standard sample is 0.51.[12]

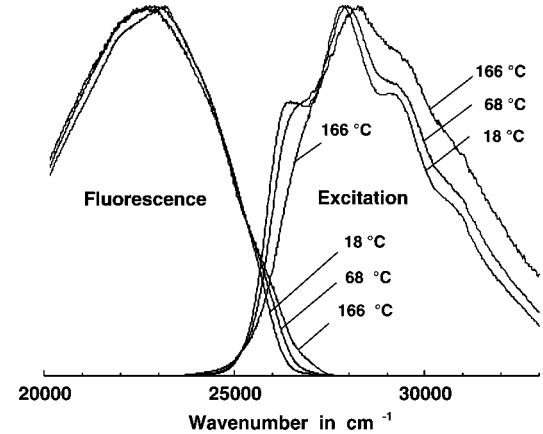

Figure 1. Corrected fluorescence and excitation spectra of DTB in dodecane at different temperatures.

3. Results

Figure 1 shows the emission and excitation spectra of DTB in dodecane at different temperatures. There is a comparatively large Stokes shift seen between the measured absorption and emission spectra. In light of the emission spectra of analogous diphenylpolyenes, most of the intensity in the emission spectra is considered to derive from the 2^1A_g (S_1) → 1^1A_g (S_0) transition, as will be explained later in more detail. Closer inspection of the emission spectra reveals a weak shoulder emission band at near 26 000 cm^{-1} on the high-energy side of the S_1 fluorescence. This weak shoulder band appears to be the mirror image of the origin of the $1^1A_g \rightarrow 1^1B_u$ absorption. Analogous weak emission bands are observed for DTB also in solvents such as methanol, cyclohexane, and *n*-hexane. The excitation spectrum for the weak shoulder emission agrees well with the measured absorption spectrum. As the temperature is raised the relative intensity and energy of the weak shoulder emission increases and the excitation spectra show a corresponding blue shift.

In the case of DTE, on the other hand, such a weak band is not observed in room temperature solution and the whole emission appears to be the mirror image of the strong $1^1A_g \rightarrow 1^1B_u$ absorption with a sufficient overlapping between the emission and absorption spectra. Further, as the temperature is raised both the emission and the excitation spectra show a slight blue shift.

Parts a and b of Figure 2 respectively show the emission and absorption spectra of DTB and DTE in solvents having different polarizabilities, all measured at 20 °C, along with those in the vapor phase in the presence of a buffer gas. The temperature of the vapor sample was kept at 150 °C so as to increase the vapor pressure of the sample. Fluorescence properties of DTB and DTE in the vapor phase are somewhat complicated, because the spectral shapes of the fluorescence and excitation spectra vary depending on the sample pressure and excitation wavelength. Therefore, perfluorohexane was added to the samples to achieve the relaxed excited states of the molecules. The details of the emission properties of DTB and DTE vapors at low pressure will be reported elsewhere.

There is a large Stokes shift seen between the measured absorption and emission spectra of DTB, in particular for those in perfluorohexane and in the vapor phase. The spectra of DTB show that as the solvent polarizability increases the weak

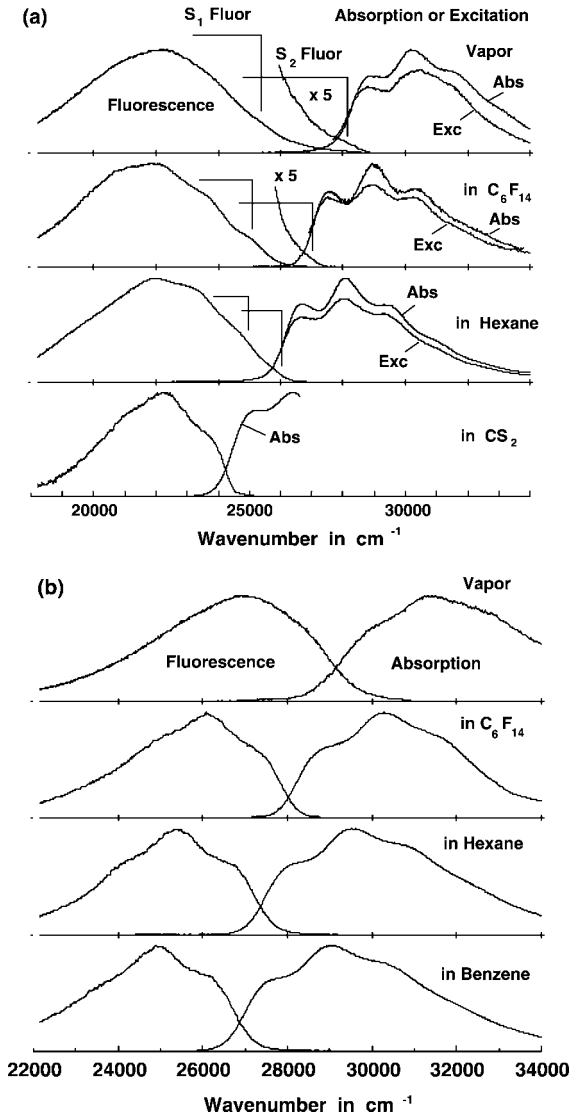

Figure 2. (a) Absorption, corrected fluorescence, and excitation spectra of DTB in different solvents at 20 °C and those in the vapor phase at 150 °C. The cutoff of the absorption spectrum of DTB in CS_2 is due to the presence of the absorption of CS_2. The excitation spectra were multiplied by 0.8 as compared with other spectra. (b) Corrected fluorescence and absorption spectra of DTE in different solvents at 20 °C and those in the vapor phase at 150 °C.

shoulder emission band shifts slightly to the red in the same way as does the absorption spectrum, except for the spectra measured in CS_2, while the position of the S_1 (2^1A_g) fluorescence remains almost constant. Further, the intensity of the weak shoulder emission increases as the position of the lowest energy band of the strong S_2 (1^1B_u) absorption shifts to the blue. These observations are similar to those reported for diphenylhexatriene and diphenyloctatetraene in room temperature solution.[13−15,17] On the other hand, the emission of DTB in CS_2 and DTE appears to be the mirror image of the strong $1^1A_g \rightarrow 1^1B_u$ absorption with a sufficient overlapping between the emission and absorption spectra. Further, as the solvent polarizability increases the emission band of DTE shifts to the red in the same way as does the absorption spectrum.

4. Discussion

The weak shoulder emission band that is seen on the high-energy side of the strong emission of DTB in room temperature solution is assigned to the S_2 (1^1B_u) → S_0 (1^1A_g) fluorescence on the basis of the following observations: (1) The weak shoulder emission band shows the expected mirror image relationship to the strong $1^1A_g \rightarrow 1^1B_u$ (S_2) absorption spectrum. (2) The excitation spectrum for the weak shoulder emission corresponds almost exactly to the $1^1A_g \rightarrow 1^1B_u$ (S_2) absorption spectrum. (3) The solvent shift behavior of the weak emission band is the same as that of the S_2 absorption, while the position of the first 2^1A_g fluorescence band is almost invariant.

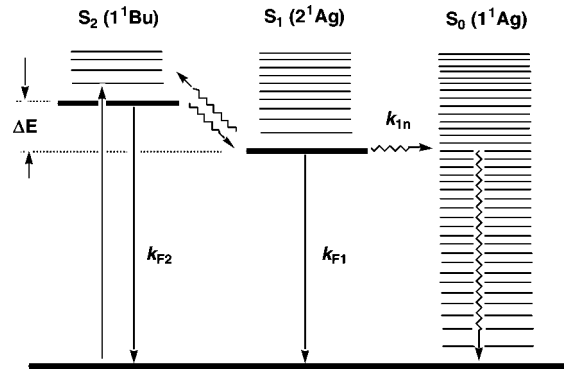

Figure 3. Kinetic scheme used to interpret the temperature and solvent dependence of the measured spectra and lifetimes of DTB.

This assignment makes it possible to quantitatively fit the dependence of the observed emission and absorption or excitation spectra as well as the fluorescence lifetimes on temperature and solvent polarizability. The general observations are that there is a weak emission band on the high-energy side of the S_1 fluorescence of DTB, that the relative intensity of this weak band increases with temperature and with solvent polarizability, and that the position of this weak band follows the S_2 absorption. This is the behavior that is expected if the weak emission band is assigned to the S_2 (1^1B_u) fluorescence. The relaxation model which we use to quantitatively interpret the observed phenomena is illustrated in Figure 3, where the S_1 and S_2 states are in thermal equilibrium and the S_2 fluorescence occurs as the result of the thermal population of the S_1 state. For the scheme in Figure 3, the ratio of the S_2 fluorescence quantum yield intensity Φ_{F2} to S_1 fluorescence quantum yield intensity Φ_{F1} is given by

$$\Phi_{F2}/\Phi_{F1} = (k_{F2}/k_{F1}) \exp(-\Delta E/kT) \quad (1)$$

where k_{F2} and k_{F1} are the radiative rate constants for the states S_1 and S_2, ΔE is the energy separation between the S_1 and S_2 zero-point levels, k is the Boltzmann constant, and T is the absolute temperature.

To determine the bands positions and intensities for the absorption and corrected S_1 and S_2 fluorescence spectra, all the spectral data have been fitted by sums of Gaussians. That is, the intensity $I(\nu)$ of the spectrum at wavenumber ν was assumed to have the following form: $I(\nu) = \sum_i I_i(\nu_i) \exp[-(\nu - \nu_i)^2/\sigma^2]$. In the case of fluorescence spectra of DTB, when seven Gaussians (the origin, one and two quanta of the symmetric C—C (1140 cm^{-1}) and C═C (1615 cm^{-1}) stretching modes, and the combination of the stretching modes) were fit to the first 4000 cm^{-1} of the corrected fluorescence spectra,[10,16] the measured and calculated spectra were almost indistinguishable from each other. To derive more accurate intensity estimates for the S_1 fluorescence, the S_0 (1^1A_g) → S_2 (1^1B_u) absorption spectrum reflected so as to match the reflected origin to the origin of S_2 fluorescence was subtracted from the measured fluorescence, and the resulting difference spectrum was refit by Gaussians to obtain the intensity of the Gaussian corresponding

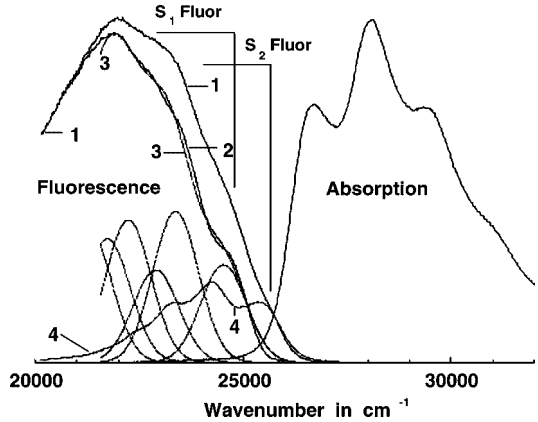

Figure 4. Absorption and corrected fluorescence spectra (1) of DTB in hexane at 20 °C. The spectra for the S_2 fluorescence (4), subtracted S_1 fluorescence (2), and fitted S_1 fluorescence (3) are shown.

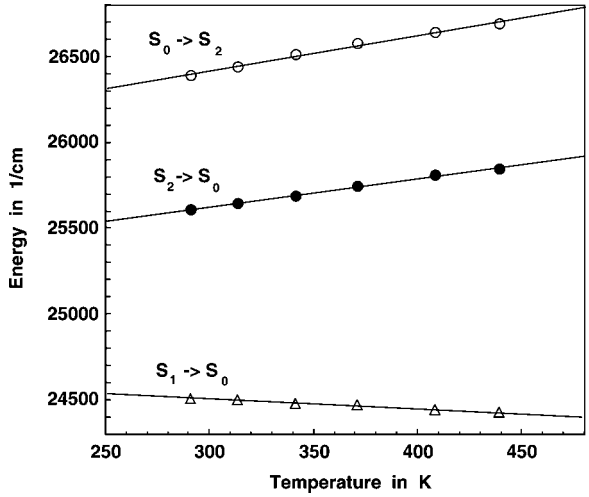

Figure 5. Band centers for the origins of the S_2 (1^1B_u) absorption ($S_0 \rightarrow S_2$), S_2 fluorescence ($S_2 \rightarrow S_0$), and S_1 (2^1A_g) fluorescence ($S_1 \rightarrow S_0$) for DTB in dodecane plotted as a function of temperature.

to the $S_1(2^1A_g)$ fluorescence alone. Examples for the subtracted and fitted S_1 fluorescence spectra of DTB in hexane are displayed in Figure 4.

4.1. Temperature Dependence of the Spectra of DTB. The fitted band positions of the S_1 and S_2 fluorescence origins and absorption or excitation origin as a function of temperature for DTB are shown in Figure 5. The S_2 fluorescence and absorption or excitation origin bands shift to the blue with increasing temperature while the position of the S_1 fluorescence origin band is almost constant. If we assume that the excitation energy decreases almost linearly with the solvent polarizability, which is approximately proportional to the reciprocal of the density, and that the density decreases nearly with increasing temperature, then we expect that the excitation energy of the S_2 level will increase approximately linearly with increasing temperature.[18] That is,

$$\Delta E = \Delta E^0 + cT \qquad (2)$$

where ΔE^0 is the energy difference between the S_1 and S_2 states at zero temperature and c is a constant. The data in Figure 5 are well fit by this relation and the slope of the S_2 fluorescence origin nearly matches that of the S_2 excitation origin, which is significantly different from that of the S_1 fluorescence origin. As is seen in Figure 1, there is a Stokes shift between the S_2 fluorescence and absorption origins. The true electronic origin

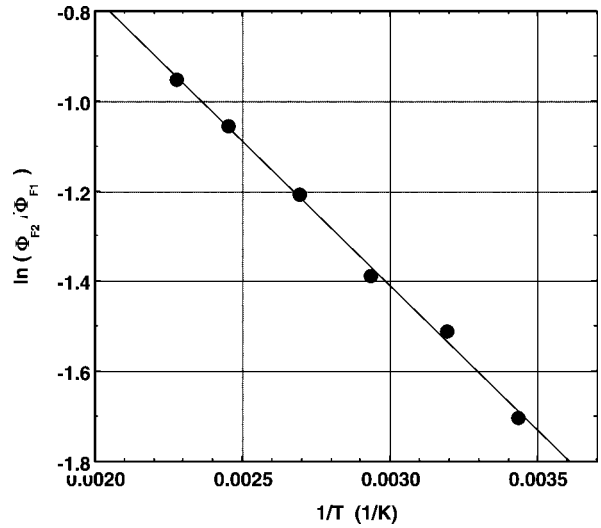

Figure 6. The logarithmic value of the ratio of the S_2 to S_1 fluorescence quantum yield plotted as a function of the reciprocal of the absolute temperature for DTB in dodecane.

for this transition lies somewhere between these two origin bands. Therefore, at temperatures near room temperature the energy difference between the observed S_2 absorption and S_1 fluorescence origin bands does not provide the true ΔE value. Thus, we have tentatively taken the energy difference between the S_1 and S_2 fluorescence origin bands as the value for ΔE.

As is seen in Figure 1, the intensity distribution in the fluorescence spectra of DTB depends on temperature. As the temperature is increased the relative intensity of the S_2 fluorescence increases. For the kinetic model shown in Figure 3, the fluorescence intensity ratio is proportional to $\exp(-\Delta E/kT)$. The logarithmic value of the ratio of the S_2 to S_1 fluorescence quantum yield is shown in Figure 6 as a function of the reciprocal of the absolute temperature. As shown by the solid lines in Figure 6, these data are well fit by this model. Since the value for ΔE also changes slightly with varying temperature, this has to be taken into account to analyze the data in Figure 6. Combination of eqs 1 and 2 provides

$$\ln(\Phi_{F2}/\Phi_{F1}) = \ln(k_{F2}/k_{F1}) - \Delta E^0/kT - c/k \qquad (3)$$

Applying eq 3 to the data in Figure 6 ($c = 2.2$ cm^{-1}/K), we obtain 450 cm^{-1} as ΔE^0 and 40 as k_{F2}/k_{F1} for DTB in dodecane. Thus, we obtain 1100 cm^{-1} as ΔE for DTB in dodecane at 20 °C, which is in reasonable agreement with the value obtained from the band locations of the fluorescence spectrum in dodecane at 20 °C ($\sim$940 cm^{-1}).

4.2. Solvent Polarizability Dependence of the Spectra of DTB. In Figure 7 we show the dependence of the origin band centers for the 1^1Ag and 1^1Bu fluorescence and the 1^1Bu absorption on solvent polarizability ($\alpha = (n^2 - 1)/(n^2 + 2)$) for solutions of DTB at room temperature. Figure 7 shows that as the solvent polarizability is increased the band position of the S_2 fluorescence origin shifts to the red as does the band position of the S_2 excitation origin, although the band position of the S_1 fluorescence maintains an almost constant value. Further, we can see that the locations of the 1^1B_u and 2^1A_g fluorescence origins invert in the solvent with the polarizability of near 0.32. This is a clear indication that in CS_2 ($\alpha = 0.354$) DTB fluoresces entirely from the 1^1B_u state, which is consistent with the observation that there is a sufficient overlapping between the emission and absorption spectra in CS_2. Therefore, in the following treatment the data for DTB in CS_2 are excluded.

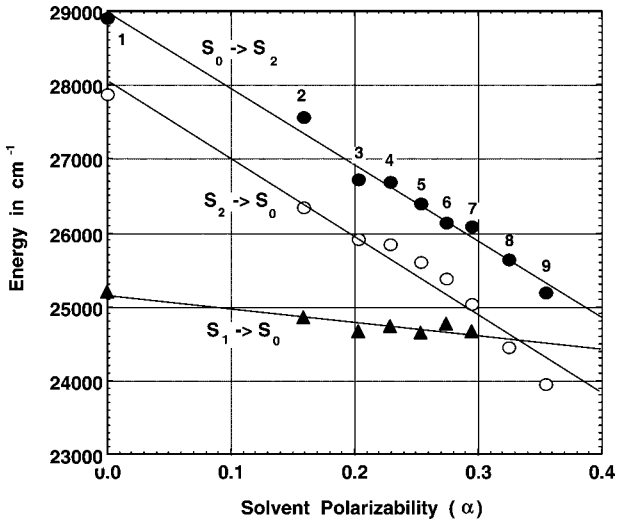

Figure 7. The dependence of the origin band centers for the 1^1A_g (closed triangles) and 1^1B_u fluorescence (open circles) and 1^1Bu absorption (closed circles) on solvent polarizability (α) for solutions of DTB at room temperature: vapor (1); perfluorohexane (2); methanol (3); hexane (4), dodecane (5); CCl_4 (6); benzene (7); benzene−CS_2 (1:1) mixture (8); CS_2 (9).

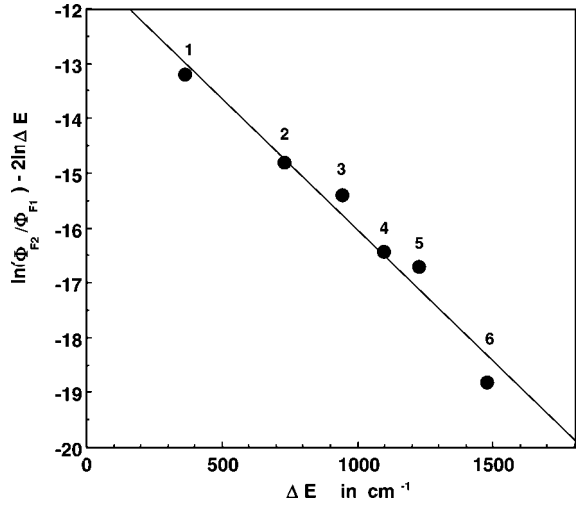

Figure 8. Values for $\ln(\Phi_{F2}/\Phi_{F1}) - 2 \ln \Delta E$ plotted against ΔE for DTE in different solvents at 20 °C. The solvents used are benzene (1), benzene−hexane (1:1) mixture (2), dodecane (3), hexane (4), methanol (5), and perfluorohexane (6).

By changing the solvent polarizability, the intensity of the S_2 fluorescence relative to the S_1 fluorescence increases as the energy difference between these bands decreases as shown in Figure 2. This phenomenon can be understood also in terms of the kinetic scheme in Figure 3. To analyze solvent polarizability dependence of the observed spectra, we have carried out more strict treatment, since the S_1-S_2 energy separation (ΔE) change with solvent polarizability is much larger than that observed in changing temperature. In eq 1, the ratio k_{F2}/k_{F1} is related to the ratio of the oscillator strength for the S_0-S_2 transition, f_{S2}, to that for the S_0-S_1 transition, f_{S1}, by $k_{F2}/k_{F1} = f_{S2}/f_{S1}$. If we assume that the radiative strength for the S_1 fluorescence originates from the coupling between the S_1 and S_2 states, the oscillator strengths should obey an expression of the from

$$f_{S1} = f_{S2}K^2/\Delta E^2 \qquad (4)$$

where K is the matrix element connecting the two excited states and may be vibronic in nature. It has been shown for

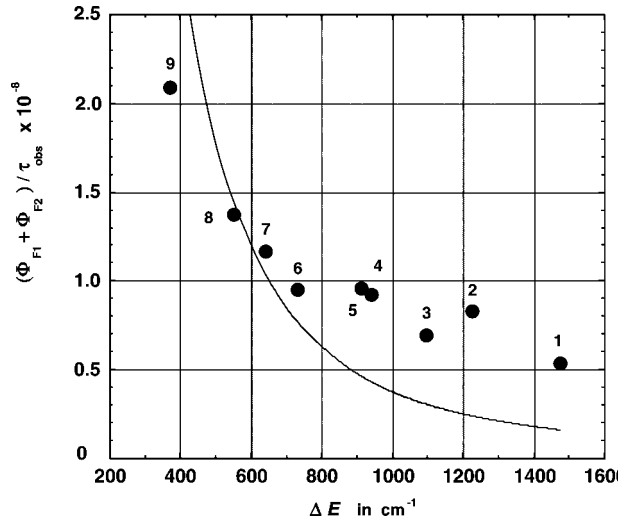

Figure 9. Values for Φ_{obs}/τ_{obs} plotted against ΔE for DTE in different solvents at 20 °C, with the precise data shown in Table 1 (The numbers correspond to those in Table 1). The solid line corresponds to the case where $K = 260$ cm^{-1} in no. 8.

TABLE 1: Fluorescence Lifetimes and Quantum Yields of DTB in Different Solvent at 20 °C

no.	solvent	τ (ns)	$\Phi_{F1} + \Phi_{F2}$	Φ_{F2}/Φ_{F1}
1	perfluorohexane	4.1	0.21	0.015
2	methanol	0.6	0.05	0.084
3	*n*-hexane	2.6	0.18	0.088
4	cyclohexane	2.7	0.23	0.178
5	methylcyclohexane	2.6	0.24	0.180
6	benzene + cyclohexane (1:2)	2.1	0.19	0.202
7	benzene + cyclohexane (1:1)	1.8	0.20	0.212
8	benzene + cyclohexane (2:1)	1.6	0.21	0.222
9	benzene	1.1	0.22	0.241

diphenylpolyenes that the coupling constant K is not a function of the solvent.[19] It follows from eqs 1 and 2 that[20]

$$\ln(\Phi_{F2}/\Phi_{F1}) = 2 \ln \Delta E - \Delta E/kT - 2 \ln K \qquad (5)$$

Hence, the slope and intercept of the plots of $\ln(\Phi_{F2}/\Phi_{F1}) - 2 \ln \Delta E$ against ΔE should provide the values for $1/kT$ and K, respectively. The experimental data were analyzed on the basis of eq 5, with the results shown in Figure 8. The plots provide a straight line as expected from eq 5 and give the k value of 0.71 ± 0.01 cm^{-1} K^{-1}, which is very close to the real Boltzmann constant of 0.6950 cm^{-1} K^{-1}. Further, the intercept of the plots provides the coupling constant K of near 280 cm^{-1}, which is of a reasonable order of magnitude for vibronic coupling energies of polyatomic molecules.[21]

4.3. Solvent Polarizability Dependence of the Fluorescence Lifetime of DTB. The molar extinction coefficient of DTB at the S_2 (1^1Bu) absorption maximum is obtained to be 19 570 in hexane at room temperature. Thus, the intrinsic radiative lifetime of the S_2 (1^1B_u) state calculated by using the Strickler−Berg equation is estimated to be 2 ns ($k_{F2} = 5 \times 10^8$ s^{-1}). Obviously, the measured fluorescence lifetimes of DTB in perfluorohexane, hexane, cyclohexane, and methylcyclohexane shown in Table 1 are longer than the estimated radiative lifetime of the S_2 state, despite the fact that the fluorescence quantum yields are less than unity. It is shown easily from the scheme in Figure 3 that

the observed fluorescence lifetime k_{obs} ($=1/\tau_{obs}$) at a particular temperature T is given approximately by

$$k_{obs} = k_{F1} + k_{ln} + k_{F2}\exp(-\Delta E/kT) = k_{F2}[K^2/\Delta E^2 + k_{ln}/k_{F2} + \exp(-\Delta E/kT)] \quad (6)$$

where k_{1n} is the nonradiative rate constant of S_1. Therefore, we obtain

$$\Phi_{obs}/\tau_{obs} = k_{F2}[K^2/\Delta E^2 + \exp(-\Delta E/kT)] \quad (7)$$

where $\Phi_{obs} = \Phi_{F1} + \Phi_{F2}$.

Figure 9 shows the values for Φ_{obs}/τ_{obs} plotted against ΔE. It is seen that the Φ_{obs}/τ_{obs} value increases with decreasing ΔE, but the agreement between the data and predicted curve is not so significant. There are mainly three reasons considered for the discrepancy between the predicted and measured Φ_{obs}/τ_{obs} values: (1) the difficulty of the evaluation of the accurate ΔE values, (2) the neglect of the contribution to the oscillator strength of the S_1 (1^1A_g) from the higher singlet states other than S_2 (2^1B_u), and (3) the difficulty of the evaluation of the accurate fluorescence quantum yields. The best-fitted value for K was obtained to be 260 ± 20 cm^{-1}, which is in excellent agreement with that estimated from the solvent polarizability dependence of the spectra (section 4.2) and is also of a reasonable order of magnitude for vibronic coupling energies of polyatomic molecules.[21]

5. Conclusions

Fluorescence, fluorescence excitation and absorption spectra, and fluorescence lifetimes have been measured for α,ω-dithenylbutadiene (DTB) and α,ω-dithenylethylene (DTE) in solvents with different polarizabilities and at different temperatures as well as in the vapor phase. It is shown that DTB exhibits the S_2 (1^1B_u) and S_1 (2^1A_g) fluorescence, with the former emission occurring through the thermal population of the S_1 state at temperatures near room temperature, while DTE exhibits only the S_1 (1^1B_u) fluorescence. That is, the S_1 state is assigned to 2^1A_g for DTB and 1^1B_u for DTE in most of the solvents: The 2^1A_g and 1^1B_u state levels of DTB invert in solvents with the polarizability α of near 0.32. Although the 2^1A_g and 1^1B_u states are nearly degenerate for DTB in a low-temperature alkane matrix,[11] the former state is located at about 2000 cm^{-1} below the latter state in alkane at room temperature. All the available information on temperature and solvent dependence of the absorption, fluorescence and excitation spectra, and fluorescence lifetime, as well as the fluorescence band locations, strongly support the presence of the lowest -lying excited singlet 2^1A_g state, which is consistent with the results obtained in low-temperature matrices.[11]

References and Notes

(1) Hudson, B. S.; Kohler, B. E. *Chem. Phys. Lett.* **1972**, *14*, 299.
(2) Hudson, B. S.; Kohler, B. E. *J. Chem. Phys.* **1973**, *59*, 4984.
(3) Hudson, B. S.; Kohler, B. E.; Shulten, K. *Excited States* **1983**, *6*, 1.
(4) Kohler, B. E. *Chem. Rev.* **1993**, *93*, 41, and references cited therein.
(5) Horwitz, J. S.; Itoh, T.; Kohler, B. E.; Spangler, C. W. *J. Chem. Phys.* **1987**, *87*, 2433.
(6) Kohler, B. E.; Spangler, C. W.; Westerfield, C. *J. Chem. Phys.* **1988**, *89*, 3506.
(7) Itoh, T.; Kohler, B. E. *J. Phys. Chem.* **1988**, *92*, 1807.
(8) Itoh, T. *J. Chem. Phys.* **2003**, *119*, 4516.
(9) Snyder, R.; Arvidson, E.; Foote, C.; Harrigan, L.; Christensen, R. L. *J. Am. Chem. Soc.* **1985**, *107*, 4117.
(10) Itoh, T. *J. Phys. Chem. A* **2007**, *111*, 3502.
(11) Birnbaum, D.; Kohler, B. E.; Spangler, C. W. *J. Chem. Phys.* **1991**, *94*, 1684.
(12) Melhuish, W. H. *J. Phys. Chem.* **1961**, *65*, 229.
(13) Alford, P. C.; Palmer, T. F. *Chem. Phys. Lett.* **1982**, *86*, 248.
(14) Itoh, T.; Kohler, B. E. *J. Phys. Chem.* **1987**, *91*, 1760.
(15) Allen, M. T.; Miola, L.; Whitten, D. G. *J. Phys. Chem.* **1987**, *91*, 6009.
(16) Negri, F.; Zgierski, M. Z. *J. Chem. Phys.* **2001**, *115*, 1298.
(17) Kohler, B. E.; Itoh, T. *J. Phys. Chem.* **1988**, *92*, 5120.
(18) Ooshika, Y. *J. Phys. Soc. Jpn.* **1954**, *9*, 594.
(19) Andrews, J. R.; Hudson, B. S. *J. Chem. Phys.* **1978**, *68*, 4587.
(20) Itoh, T. *Chem. Phys. Lett.* **1989**, *159*, 263.
(21) Hochstrasser, R. M. *Acc. Chem. Res.* **1968**, *18*, 266.

JP804592M